Environmental Science & Technology

Perspective

Cite This: Environ. Sci. Technol. 2020, 54, 76−84

pubs.acs.org/est

Energy Efficiency of Desalination: Fundamental Insights from Intuitive Interpretation

Shihong Lin*,†,§

†Department of Chemical and Biomolecular Engineering §Department of Civil and Environmental Engineering Vanderbilt University, Nashville, Tennessee 37235-1831, United States

Supporting Information

ABSTRACT: Desalination has become an essential toolset to combat the worsening water stress resulting from population and industrial growth and exacerbated by climate change. Various technologies have been developed to desalinate feedwater with a wide spectrum of salinity. While energy consumption is an important consideration in many desalination studies, it is challenging to make (intuitive) sense of energy efficiency due to the different mechanisms of various desalination processes and the very different separations achieved. This perspective aims to provide an intuitive, thermodynamics-based interpretation of energy efficiency by illustrating how energy consumption breaks down into minimum energy of separation and the irreversible energy dissipation. The energy efficiencies of different desalination processes are summarized and rationalized based on their working mechanisms. Notably, a new concept called the *minimum mean voltage* is proposed as a convenient tool to evaluate the energy efficiency of electrochemical desalination processes. Lastly, the intrinsic trade-off between energy efficiency and desalination rate and the relevance of energy efficiency in different desalination applications are discussed.

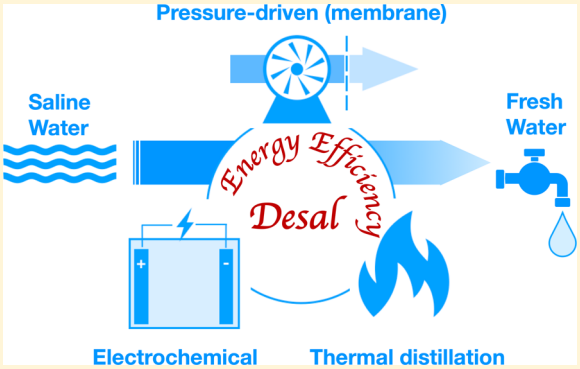

INTRODUCTION

Desalination has been extensively investigated and employed for augmenting freshwater supply and reducing the environmental impacts of saline industrial wastewater.[1] A variety of desalination technologies have been applied to feedwaters with a wide range of salinity, from wastewater reclamation and desalination of brackish groundwater to seawater desalination to the treatment of hypersaline brine.[2−4] While energy consumption is not the only important consideration in desalination practices, it is undoubtedly one of the most investigated metrics in desalination research.[5−10] Because energy consumption strongly depends on feed salinity and the degree of salt removal, more fundamental insights can be derived from energy efficiency that accounts for the intrinsic "difficulty" of desalination processes.

This perspective aims to provide an overview and an intuitive interpretation of the energy efficiency of mainstream desalination processes that are driven by pressure, electric field, and heat. After a brief description of the working mechanisms of major desalination technologies, the definition of energy efficiency is provided, and the energy efficiencies of major desalination technologies are summarized and justified with intuitive theoretical interpretations. While more rigorous and in-depth theoretical analyses on specific desalination processes are available elsewhere,[10−14] the goal of this perspective is to enable an intuitive understanding of the energy efficiency of desalination processes without resorting to the formality of thermodynamics. Interested readers are referred to classic literature for a rigorous treatment of desalination thermodynamics,[14] or holistic discussion of the energy issues in desalination.[6]

OVERVIEW OF MAINSTREAM TECHNOLOGIES

Most existing desalination technologies fall into three major categories. The first category is pressure-driven desalination, including reverse osmosis (RO) and nanofiltration (NF). In pressure-driven desalination, hydraulic pressure is applied to push the water in the feed solution through a semipermeable membrane that rejects the solutes(Figure 1a).[15] The applied pressure must exceed the osmotic pressure difference between the feedwater and the permeate to produce any water. RO typically has near-perfect rejection for charged solutes and is widely used in seawater and brackish water desalination. In contrast, NF rejects solutes to variable extents depending on the solute species, membrane properties, and operation conditions.[16]

The second category of desalination is driven by an applied voltage, with representative examples being electrodialysis, ED, and capacitive deionization, CDI (Figure 1b). In ED, ions are removed from the feedwater as they transport across ion-exchange membranes (IEMs) to the brine stream under an

Received: August 8, 2019
Published: December 9, 2019

DOI: 10.1021/acs.est.9b04788
Environ. Sci. Technol. 2020, 54, 76−84

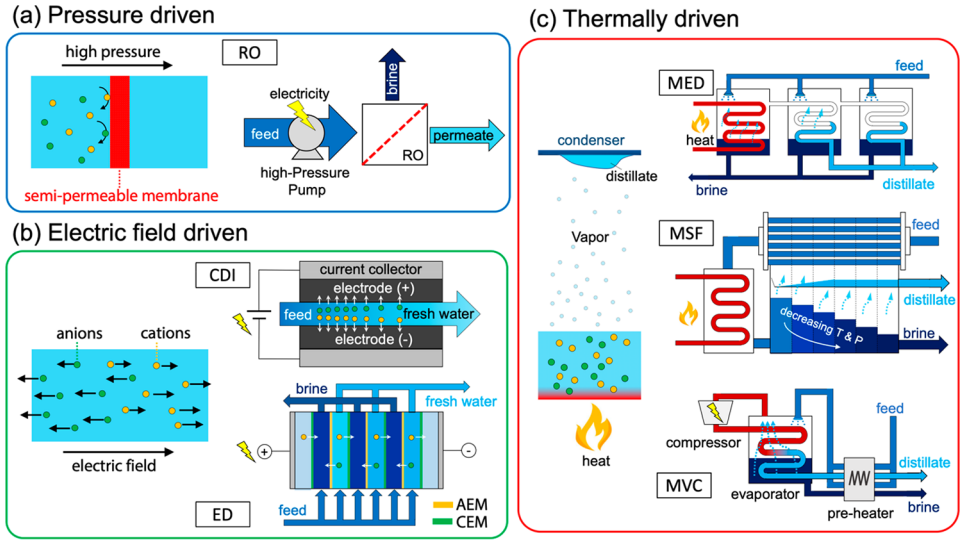

Figure 1. Schematic illustration of the three major categories of desalination processes: (a) Pressure driven desalination, such as RO or NF. (b) Electric field-driven desalination (or electrochemical desalination), such as CDI or ED. (c) Thermally driven desalination, such as MED, MSF, MVC, or membrane distillation (not shown here). All thermally driven processes involve liquid-to-vapor phase change, although the only form of external energy source of MVC is electricity.

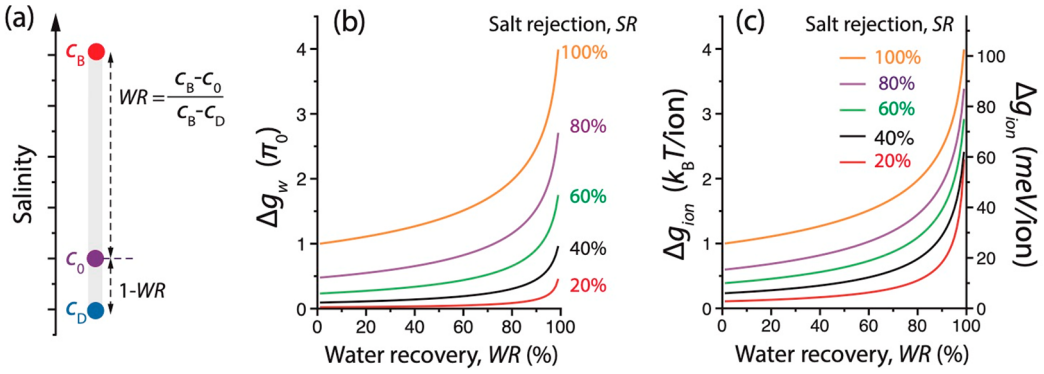

Figure 2. (a) A "separation bar" defining a desalination process. Note that WR and SR can both be defined using the three concentrations on the "separation bar". (b) Product water-specific Gibbs free energy (in the unit of feedwater osmotic pressure) as a function of WR and SR, plotted using eq 1. (c) Ion-specific Gibbs free energy (in the unit of k_BT or meV per ion) as a function of WR and SR, plotted using eq 2. In three panels, the feedwater is simplified as an ideal solution of a single-species strong electrolyte.

applied electric field. Consequently, the water in the product water channels is deionized, and the feedwater in the brine channels becomes concentrated.[17,18] In CDI, ions are removed from the feedwater via one of the two following mechanisms. The first involves the formation of electrical double layers (EDLs) on the surface of carbon electrodes with a large specific area.[19] The second involves the reaction of ions with electrode materials or the intercalation of ions into the electrode crystal lattice.[20] Most CDI processes use film-electrodes and comprise distinct charging and discharge steps, although flow-electrodes have also been explored to enable steady-state operation and higher salinity reduction.[21,22]

The third major category of desalination technology is thermal distillation, which involves the vaporization of feedwater and the subsequent condensation of the vapor to obtain distilled water (Figure 1c).[23] The three distillation-based technologies adopted widely in practical applications are multistage flash distillation (MSF), multieffect distillation (MED), and mechanical vapor compression (MVC). In MSF and MED, heat is the primary energy input, although electricity is also consumed for flow circulation and maintaining a partial vacuum.[24] While the detailed configurations of MSF and MED differ, they are both designed to enhance the recovery of the latent heat of condensation which is critical to achieving high energy efficiency. In MVC, water vapor is mechanically compressed to increase its temperature and pressure, and the latent heat from condensing the compressed vapor is reused for feed stream vaporization.[25] Unlike MSF or MED, MVC typically only consumes electricity and does not require an external heat source. Membrane distillation, an emerging and actively explored desalination technology based on partial pressure-driven vapor transport through hydrophobic membranes,[26] also falls into this third category.

GENERAL THERMODYNAMICS OF DESALINATION

For simplicity, all discussion in the following analysis is based on a single-species ideal solution of a strong electrolyte. With such an assumption, a desalination process can, in theory, be described using the molar concentrations or salinities of the feedwater (c_0), brine (c_B), and deionized product water (c_D). Conceptually, a separation can be illustrated by a "separation bar" shown in Figure 2a. The two other typical dimensionless

DOI: 10.1021/acs.est.9b04788
Environ. Sci. Technol. 2020, 54, 76−84

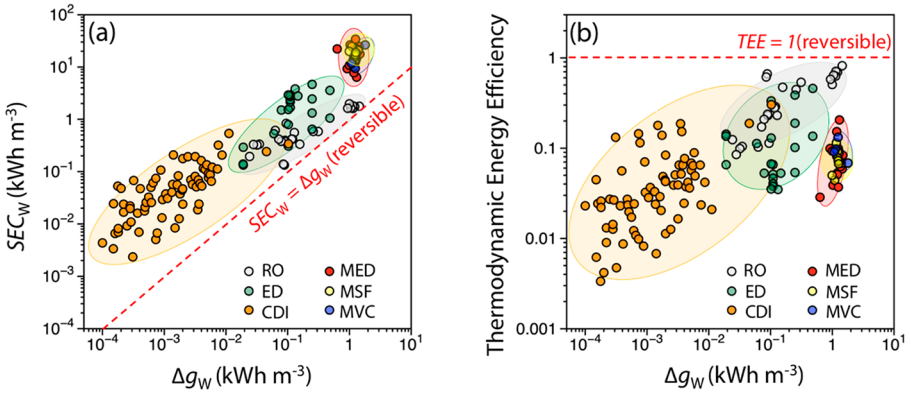

Figure 3. (a) SEC_W vs Δg_W, and (b) TEE vs Δg_W, for the major desalination technologies presented in Figure 1. In both panels, the dotted lines represent general performance limits achievable only with thermodynamically reversible processes. Note that the data used for calculation here is extracted from studies at different scales for technologies at different levels of maturity. Because the calculations only focus on the "separation step" and minimizes the consideration of any energy consumption in auxiliary processes (e.g., pretreatments), SEC_W and TEE do not necessarily represent plant-scale performance. Methodologies and references used to construct this figure are presented in SI S8.

parameters of desalination include salt rejection (SR) and water recovery (WR), which can be expressed using the three salinities (i.e., SR = $1 - c_D/c_0$, and WR = $(c_B - c_D)/(c_B - c_0)$, see Supporting Information (SI) S1).

Thermodynamics of ideal solution suggests that any separation requires a minimum amount of energy.[27] As desalination is typically an isothermal and isobaric separation (defined based on the initial and final states), this minimum energy is essentially the Gibbs free energy of separation, which is consumed by any thermodynamically reversible desalination process. Because the goal of desalination in most cases is to produce deionized water, the product water-specific Gibbs free energy, that is, the Gibbs free energy per volume of product water (Δg_w), is of particular interest. If we normalize Δg_w by the feed osmotic pressure, π_0, the result is simply a function of SR and WR (see SI S2 for derivation):

$$\frac{\Delta g_w}{\pi_0} = \frac{1}{WR}\ln\left[\frac{1 - WR(1 - SR)}{1 - WR}\right] - (1 - SR)\ln\left[\frac{1 - WR(1 - SR)}{(1 - SR)(1 - WR)}\right] \quad (1)$$

Note that the impact of solution composition and nonideality on Δg_w can be accounted for by replacing concentrations with activities as reported in literature.[28]

For electric field-driven desalination, such as ED and CDI, where ions migrate in an electric field, the Gibbs free energy of separation per ion, or the ion-specific Gibbs free energy, Δg_{ion}, provides additional insights. It can be obtained by dividing the Gibbs free energy by the number of ions transferred from one portion of the feedwater (that becomes the deionized water) to another portion of the feedwater (that becomes the brine):

$$\Delta g_{ion}(WR, SR) = \frac{\Delta g_w(WR, SR)}{SR}\frac{kT}{\pi_0} \quad (2)$$

where k is the Boltzmann constant, T is the absolute temperature. Specifically, Δg_{ion} represents the minimum energy to transfer an ion in a given separation, regardless of its charge. An interesting observation emerges from eq 1 and 2, that Δg_{ion} for ideal solutions is independent of feed salinity but only dependent on the dimensionless metrics WR and SR. This interesting observation is unsurprising though: as a heuristic example, the Donnan potential across an IEM depends only on the *ratio* between the concentrations of a charged species on two sides of the IEM, not on the absolute concentrations.[29]

The presentation of Δg_{ion} using the unit of milli-electronvolt, meV (Figure 2c) is of fundamental significance. For separating a general electrolyte = $M_{\nu+}X_{\nu-}$ that dissociates into cations M^{z^+} and anions X^{z^-}, a new concept called the *minimum mean voltage* for a reversible separation, $\overline{\Delta V_R}$(WR,SR), can be defined (see SI S3 for derivation):

$$\overline{\Delta V_R}(WR, SR) = \frac{\nu\Delta g_{ion}(WR, SR)}{|\nu^+ Z^+|e} = \frac{\nu\Delta g_{ion}(WR, SR)}{|\nu^- Z^-|e} \quad (3)$$

where ν is the van't Hoff factor for the solute ($\nu = \nu^+ + \nu^-$). An electrochemical desalination processes can only be energy-efficient if the mean voltage, $\overline{\Delta V_{cell}}$, is sufficiently close to $\overline{\Delta V_R}$(WR,SR). In the ideal case with a perfect charge efficiency, $|\nu^+ Z^+|\overline{\Delta V_{cell}}$ is simply the energy consumed to move one "ion pair" from the feedwater to the brine. The concept of minimum mean voltage facilitates convenient interpretations of energy efficiency for electrochemical desalination. For example, if a $\overline{\Delta V_{cell}}$ of 1 V is applied for a separation that only requires a $\overline{\Delta V_R}$(WR,SR) below 80 mV (e.g., NaCl solution, WR = 80%, SR = 80%), the energy efficiency cannot exceed 8% even with perfect charge efficiency. The interpretation of energy efficiency for CDI and ED will be further elaborated in later discussion.

THERMODYNAMIC EFFICIENCY OF DESALINATION TECHNOLOGIES

The energy efficiency of any desalination process can be quantified using thermodynamic energy efficiency, TEE, which is also referred to in thermodynamics as second-law efficiency or exergy efficiency.[14] TEE is quantitatively defined as the ratio between the specific Gibbs free energy and the specific energy consumption (SEC). Similar to specific Gibbs free energy, SEC can also be computed in two ways. The product water-specific energy consumption, SEC_w, is the energy consumed to generate a unit volume of deionized water; whereas the ion-specific energy consumption, SEC_{ion}, is the energy consumed to transport an ion. Using either definition, TEE can be expressed as

$$TEE = \frac{\Delta g_w}{SEC_w} = \frac{\Delta g_{ion}}{SEC_{ion}} \quad (4)$$

DOI: 10.1021/acs.est.9b04788
Environ. Sci. Technol. 2020, 54, 76−84

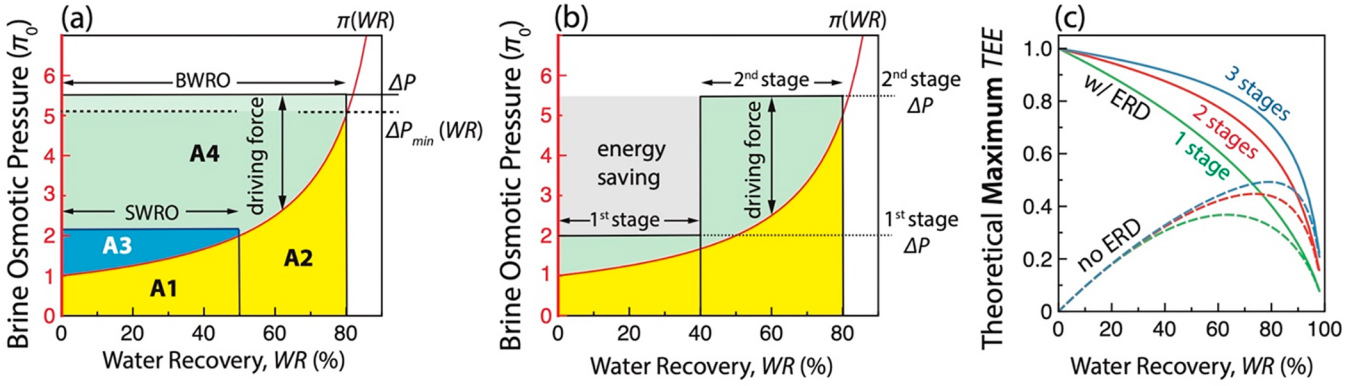

Figure 4. (a) Breakdown of energy consumption in a single-stage, continuous-flow, constant-pressure RO process for seawater RO (SWRO, lower WR) and brackish water RO (BWRO, higher WR). The red curve represents the osmotic pressure of the remaining brine after a certain fraction (WR) of the feedwater has been recovered. The difference between the applied pressure, ΔP, and the brine osmotic pressure at a specific WR is the local driving force. For a specific WR, the average height of the yellow region (bounded by that WR) is Δg_W. For SWRO, Δg_W, and SEC_W correspond to the average heights of the regions A1 and A1+A3, respectively. For BWRO, Δg_W and SEC_W correspond to the average heights of the regions A1+A2 and A1+A2+A3+A4, respectively. (b) Breakdown of energy consumption in a two-stage, BWRO process. The energy-saving by a two-stages RO process is illustrated by the area of the gray region. (c) Theoretical maximum TEE as a function of WR with for RO processes with different stages, with (solid curves) and without (dash curves) energy recovery device. The detailed derivations and explanations of Figure 4 are presented in the SI.

For thermal desalination with heat as the primary energy input, the definition of SEC is not based on the primary heat energy input but rather the equivalent work extractable from such heat input assuming a perfect heat-to-work conversion with Carnot efficiency.

The values of Δg_w,SEC_w, and TEE for different desalination processes evaluated from the literature are summarized in Figure 3. The data for CDI is mostly from a recent review paper by Wang et al.,[30] whereas the data for other desalination processes are extracted from other papers (refer to the methodologies in SI S8 for the assumptions made in data extraction). While effort has been made to include as much representative data as possible, this summary is not meant to be exhaustive. In general, CDI has relatively low Δg_w resulting from partial desalination of low salinity feedwater. The majority of Δg_w for documented CDI processes ranges from 10^{-4} to 10^{-2} kWh m^{-3}, although CDI using intercalation materials as electrodes has been applied for seawater desalination with Δg_w up to ~0.1 kWh m^{-3}.[31]

In comparison, ED and RO reported in literature achieved higher Δg_w ranging from ~0.02 to 0.48 kWh m^{-3} for ED and from ~0.02 to 1.45 kWh m^{-3} for RO. As the state-of-the-art desalination technology, RO has been applied for desalinating feedwater with a wide range of salinity, including seawater, brackish water, and treated wastewater. While a theoretical analysis comparing RO and CDI has been performed in a recent study,[32−34] no sufficient experimental data could be found in literature to calculate the TEE of RO for treating very low-salinity feedwater typically treated by CDI. Thermal desalination processes such as MED, MSF, and MVC are all characterized by high Δg_w that are typically above 1.0 kWh m^{-3} (up to 1.8 kWh m^{-3}).

The summarized data suggests SEC_w positively correlates with Δg_w for pressure-driven and electrochemical desalination (Figure 3a). The data points for RO are closer to the line corresponding to thermodynamically reversible processes (i.e.,$SEC_w = \Delta g_w$), suggesting that RO is generally more energy efficient. The data in Figure 3a can be converted to a figure showing TEE vs Δg_w (Figure 3b), which shows that TEE also positively correlates with Δg_w for nondistillation desalination processes, that is, it is generally easier to achieve a higher TEE for "more difficult" separations with higher Δg_w.

Overall, RO is currently the most energy-efficient desalination technology in terms of TEE, although the conclusion is drawn from data in a limited range of relatively high Δg_w. In the similar range of Δg_w, ED seems to be less efficient than RO. Thermal distillation processes are relatively inefficient and only applied to achieve separations with very high Δg_w. The available data for CDI suggests that CDI generally has low TEE, but in exceptional cases with the highest Δg_w, can also achieve TEE comparable with that for RO and ED.

INTUITIVE INTERPRETATION OF ENERGY EFFICIENCY

The summary of TEE from experimental studies is only empirically informative. It does not elucidate why some desalination processes are more efficient than the others, nor does it reveal the potential and strategies to enhance TEE. Without resorting to detailed and rigorous process modeling, simplified analyses of energy efficiency for individual desalination processes are presented here to impart intuitive interpretation of TEE.

Reverse Osmosis. Let us start with RO as it is a simple yet currently the most energy-efficient desalination process. In the simplified case with perfect salt rejection (i.e., SR = 100%), the brine osmotic pressure is a simple function of WR and the feed osmotic pressure, $\pi(WR) = \pi_0/(1 - WR)$ as shown in the red curve of Figure 4a). A *batch* RO process can be performed reversibly by applying a hydraulic pressure that is infinitesimally higher than the trans-membrane osmotic pressure difference. With such a reversible path, SECw is simply the WR-weighted average brine osmotic pressure as represented by the average height of the yellow region in Figure 4a. Theoretical proof has been provided that SEC_w of such a reversible RO process exactly equals Δg_w.[35,36]

However, most practical RO processes are operated using a continuous flow system with constant pressure (CP). For a single-stage, constant-pressure, and continuous flow RO process, SEC_w is simply the applied hydraulic pressure if a

DOI: 10.1021/acs.est.9b04788
Environ. Sci. Technol. 2020, 54, 76−84

perfectly efficient energy recovery device (ERD) is employed to recover the mechanical energy in the pressurized brine stream. In this case, the theoretical maximum TEE, or TEE_{max}, can be expressed as

$$TEE_{max} = \frac{1 - WR}{WR} \ln\left(\frac{1}{1 - WR}\right) \quad (5)$$

The assumption of a perfect ERD is reasonable for state-of-the-art seawater RO (SWRO). For brackish water RO (BWRO) with high WR, ERD is not necessary because only a small fraction of the feedwater is rejected as brine. When ERD is not employed, the maximum TEE with "no recovery", $TEE_{NR,max}$, becomes

$$TEE_{NR,max} = (1 - WR) \ln\left(\frac{1}{1 - WR}\right) \quad (6)$$

The derivation of both eq 5 and 6 is presented in SI S4. In both equations, the maximum TEE is achieved when the lowest allowable pressure is applied to achieve a target WR (i.e., $\Delta P = \pi(WR)$). In practical RO processes, however, ΔP is slightly higher than π(WR) to maintain finite driving force throughout the module.

For SWRO that typically achieves a WR below 50%, TEE is easily over 60% for the separation step assuming a perfect ERD, as the "excess energy" for providing the driving force (A3 in Figure 4a) is relatively small compared to the minimum energy for separation (A1 in Figure 4a). Such "excess energy," which is essentially $SEC_w - \Delta g_w$, results in entropy generation and should be minimized for achieving a high TEE. TEE becomes much lower for single-stage RO processes with very high WR (e.g., BWRO) as the excess energy (A3+A4 in Figure 4a) becomes significant compared to Δg_w (A1+A2 in Figure 4a), which is attributable to the rapid increase of π(WR) with increasing WR when WR approaches 100%.

A simple way to enhance the TEE of BWRO with high WR is to implement staging to reduce the average driving force. For example, if a BWRO process with WR = 80% is performed using two stages each recovering product water at an equal flow rate, the overall excess energy and SECw can be significantly reduced (as quantified by the gray area in Figure 4b). Notably, staging saves energy with and without ERD (Figure 4c, with derivation detailed in SI S4). Recent studies have also examined batch or closed-circuit RO for energy saving via creating more temporally uniform driving force.[36−39]

Overall, the above analysis clearly illustrates why RO is intrinsically energy efficient. The reversible path of RO operation dictates that a relatively small fraction of energy is consumed to provide the driving force which results in entropy generation. This interpretation is valid as long as feed salinity is not too low. When the feed salinity is so low that π_0 becomes negligible compared to the minimum pressure required to overcome membrane resistance and hydraulic resistance along the module, TEE of RO may become very low.

Electrochemical Desalination. Although both driven by an applied voltage, ED and CDI have different distributions between Δg_w (yellow regions in Figure 5a,b) and excess energy (red regions in Figure 5a,b). For processes based on electric field-driven ion transport, the analysis is most convenient by showing the cell voltage against the amount of transferred charge (in Coulomb or mole). For ED, the thermodynamically reversible path is characterized by a variable cell voltage that always equals the equilibrium voltage, that is, the sum of the

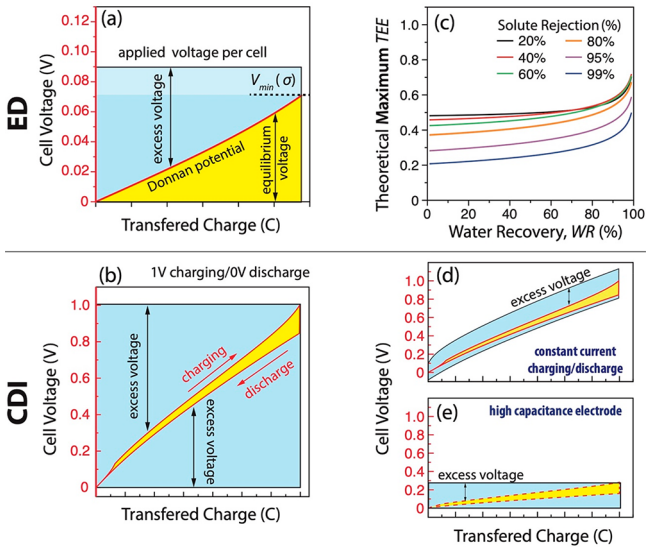

Figure 5. Breakdown of energy consumption in (a) a single-stage ED process and (b) a CDI process with constant voltage charging and zero voltage discharge (CV/ZV). In both cases, the red curves represent the thermodynamically reversible paths, whereas Δg_{ion} and SEC_{ion} correspond to the average height of the yellow regions and the height of the blue rectangles, respectively. (c) Theoretical maximum TEE as a function of WR and SR for a single-stage ED process. Here, maximum TEE is achieved when the cell voltage equals the "final" equilibrium voltage (i.e., driving force becomes zero at the exit of the module). (d) Illustration of how constant current charging and discharge improves TEE. (e) Illustration of how electrodes with higher capacitance improve TEE even with CV/ZV operation mode. The numerical values are deliberately omitted in panels (a), (b), (d), and (e), as they are strongly case-dependent (details are given in SI S5).

Donnan potentials across all IEMs. The Donnan potential across an IEM, being a function of the ratio of ion concentrations on both sides of the IEM, depends on the extent of charge transfer. Such a reversible process can only be achieved using a batch system with infinitesimal current density. Single-stage, continuous-flow ED process only has a single cell voltage, which must equal or exceed the "final" equilibrium voltage (i.e., at the exit of the module) corresponding to the extent of charge transfer required for achieving a target separation. For a Z^+: Z^- electrolyte, the final equilibrium voltage for one pair of IEMs, $V_{cell,eq}$(WR,SR), depends only on WR and SR, following the equation below (see SI S6 for derivation):

$$\frac{eV_{cell,eq}(WR, SR)}{kT} = \left(\frac{Z^+ + Z^-}{Z^+Z^-}\right) \ln\frac{1 - WR(1 - SR)}{(1 - WR)(1 - SR)} \quad (7)$$

The minimum mean voltage introduced in eq 3, $\overline{\Delta V_R}$(WR,SR), is equivalent to the average height of the yellow region in Figure 5a. Consequently, TEE for a single-stage ED process (assuming perfect current efficiency) is the ratio between $\overline{\Delta V_R}$(WR,SR) and the applied cell voltage, ΔV_{cell}, which is graphically the area ratio between the yellow region and the rectangle with a height of ΔV_{cell} (Figure 5a). Maximum TEE for a single-stage ED process achieving a specific separation is attained when ΔV_{cell} equals $V_{cell,eq}$ (i.e, zero driving force at the exist of the module). The theoretical maximum TEE for a single-stage ED, being the ratio of $\overline{\Delta V_R}/V_{cell,eq}$, can easily achieve a double-digit value regardless of WR and SR (Figure

DOI: 10.1021/acs.est.9b04788
Environ. Sci. Technol. 2020, 54, 76−84

5c). Contrary to single-stage RO, which has lower TEE at higher WR, TEE of ED slightly improves with higher WR. However, for seawater desalination which requires reducing the salinity from 35 g L^{-1} by ~99%, ED (Figure 5c) is intrinsically less efficient than RO with ERD (Figure 4c) unless RO is pushed to achieve an ultrahigh WR. Notably, the maximum TEE shown in Figure 5c are indeed the upper bound when compared to ED with the highest TEE in literature (Figure 3b).

The analysis of TEE for CDI has been presented in a recent paper by Wang et al.,[30] and will be illustrated here using an example where an CDI cell with activated carbon is charged at constant voltage (1 V) and discharged by short-circuiting (i.e., 0 V) to achieve the same separation characterized by a thermodynamically reversible charging/discharge cycle highlighted in yellow in Figure 5b. Note that SEC_w of such a reversible CDI cycle has been shown to be exactly Δg_w.[40−42] In this case, TEE is the ratio between the area of the yellow cycle and that of the rectangle encompassing the yellow cycle (Figure 5b). Alternatively, we can also calculate the minimum mean voltage, $\overline{\Delta V_R}$(WR,SR) which is ~62 mV for separating a 1:1 electrolyte with WR = 50% and SR = 95%, according to eq 3. Note that 62 mV here is essentially the average height of the yellow cycle in Figure 5b. If a CDI cell is charged at 1 V and discharged at 0 V (i.e., CV/ZV mode), $\overline{\Delta V_{cell}}$ is 1 V and TEE is capped at ~6.2%. The two approaches of quantifying TEE, one using the "area ratio" in Figure 5b, the other using the ratio between $\overline{\Delta V_R}$(WR,SR) and $\overline{\Delta V_{cell}}$, are fundamentally equivalent.

This intuitive interpretation of TEE sheds light on the general strategies for making CDI more energy-efficient, as illustrated here using two examples. In the first example, the same separation as in Figure 5b is now achieved by constant current charging and discharge.[9,43] If the cell resistance and current density are both low, and the energy released in discharge can be fully recovered, the excess energy can be significantly reduced (Figure 5d vs b). In the second example where electrodes with high capacitance (e.g., more electrode mass per area or electrode made of intercalation materials) are used, the cell voltage rise can be much lower for storing the same amount of charge (as required for achieving the same separation). In this case, $\overline{\Delta V_{cell}}$ can also be substantially reduced even if the cell is operated in CV/ZV mode (Figure 5e). In both cases, a higher TEE is achieved because $\overline{\Delta V_{cell}}$ is reduced while $\overline{\Delta V_R}$(WR,SR) remains the same for a specific separation.

Thermal Distillation. Thermal distillation is inherently energy-intensive due to the presence of phase-change. The vaporization enthalpy, H_{vap}, is typically orders of magnitude higher than Δg_w of the resulting salt-water separation. TEE of a general thermal distillation process can be quantified using the following eq (SI S7 for detailed derivation)

$$\mathrm{TEE} = \frac{1}{H_{vap}\eta_{Carnot}}\frac{1}{\mathrm{WR}}\ln\left(\frac{1}{1-\mathrm{WR}}\right)\pi_0\mathrm{GOR} = \zeta\pi_0\mathrm{GOR} \quad (8)$$

where GOR is the gained-output-ratio that roughly quantifies how many times latent heat of condensation is reused,[10,44] η_{Carnot} is the Carnot efficiency, and ζ is a coefficient that integrates the H_{vap}, η_{Carnot}, and the WR-dependent terms. A simple analysis (SI S7) suggests that ζ has a relatively narrow range of values in most practical situations, which contrasts π_0 and GOR that can vary in much larger ranges. With working temperatures of 80 and 20 °C, and a WR of 60%, ζ has a value of around 0.014 m^3 kwh^{-1}.

For thermal distillation processes to achieve a high TEE, they must be used to desalinate feedwater with high salinity (i.e., large π_0) and achieve a high level of latent heat recovery (i.e., high GOR). For example, with seawater ($\pi_0 \approx$ 0.76 kWh m^{-3}) as the feedwater and a GOR of 10 (typical of large-scale MSF and MED plants), a TEE of 10% can be achieved. Higher TEE is expected for desalination of hypersaline brine.

TRADEOFF BETWEEN ENERGY EFFICIENCY AND DESALINATION RATE

An intrinsic trade-off exists between energy efficiency and desalination rate, as it consumes more energy to drive faster desalination. Typically, the desalination rate can be tuned by adjusting the driving force for mass or charge transfer, such as the excess pressure in RO (Figure 4a) and the excess voltage in ED (Figure 5a) and CDI (Figure 5b,c,d).[13,45−47] In MSF and MED, the fundamental driving force is the partial vapor pressure difference, and the proxy driving force is the temperature difference.[10] Adding more stages/effects without changing the overall working temperatures enhances GOR and TEE but at the cost of reducing the driving force (i.e., the temperature difference per stage/effect) and thus the desalination rate.

This universal trade-off suggests that one can always reduce energy consumption at the cost of desalination rate, which can be described by a trade-off curve plotting the inverse of SEC (i.e., SEC^{-1}) over a range of desalination rate for the same separation (Figure 6a).[45−48] A trade-off curve represents a set of coupled design and operation conditions with which the target separation can be achieved. The presence of such a trade-off also suggests that comparing the energy consumption of two desalination processes is not truly meaningful unless they have the same desalination rate. Practically, because a lower desalination rate requires a larger system to achieve the same production capacity, the technical trade-off between energy efficiency and desalination rate can translate to an economic trade-off between energy cost and the system size-dependent capital cost. Therefore, a trade-off curve can also serve as the technical basis for process economic optimization.

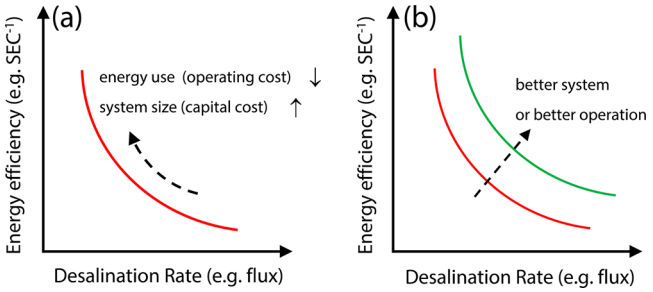

Figure 6. (A) Illustration of the trade-off between energy efficiency and desalination rate. The energy efficiency can be quantified by the inverse of SEC (i.e., SEC^{-1}) and the definition of desalination rate is highly system dependent (e.g. flux for membrane processes). (B) a desalination system or operation is better if it results in a "higher" trade-off curve corresponding to the same separation as achieved by the system or operation being compared.

Comparative assessment between two systems using the same desalination technology may be performed by comparing the positions of the corresponding trade-off curves (Figure

DOI: 10.1021/acs.est.9b04788
Environ. Sci. Technol. 2020, 54, 76−84

6b).[45−48] Comparison across technological platforms is technically tricky because even the quantitative definitions of desalination rate and system size vary between different technologies. In this case, cross-technology comparison cannot be conducted directly using performance trade-off curves but should use the minimum levelized cost of water estimated from these trade-off curves via proper cost models.

CONCLUDING REMARKS

Energy consumption is typically a major consideration in desalination research. While specific energy consumption is of direct practical relevance, TEE is a more fundamental metric that accounts for the intrinsic "difficulty" of the separation. I hope that the readers acquire an intuitive understanding of TEE through the graphical illustrations of how energy consumption in different desalination processes breaks down to the energy intrinsically required for the separation and the excess energy driving the mass transfer. For nonthermal desalination processes, such a breakdown is primarily dependent on the shape of the thermodynamic reversible path and the operation mode.

In theory, all nonthermal desalination processes can be energy efficient because they spend the energy directly on saltwater separation instead of inducing phase-change. However, due to the typically small Δg_w and a large amount of energy stored in the charging stage, attaining a high TEE for CDI with activated carbon electrodes is practically challenging. Enhancing TEE of CDI requires reducing the excess voltage, which may be achieved via using high capacitance electrode (e.g., more AC electrode mass per area, or electrodes made of intercalation materials) and optimizing operation (e.g., reducing current density and maximizing energy recovery in discharge). For thermal desalination to achieve a reasonable TEE, latent heat recovery is critical, and the process must be employed to desalinate high-salinity feedwater.

For seawater desalination which currently has the largest market, RO is the most mature and competitive technology. The evolvement of RO to become the leading seawater desalination technology over the past decades has a rather strong theoretical basis as illustrated in Figure 4a, and its dominance in seawater desalination is unlikely challenged in any near future. ED is not as widely adopted as RO in seawater desalination not only because the cost of IEMs is substantially higher than RO membranes but also because its intrinsic energy efficiency cannot compete with RO. Due to the inherent limitation in energy efficiency, thermal distillation technologies have dwindled in the market of seawater desalination over the past few decades.[3]

For desalinating low-salinity feedwater, such as brackish groundwater and treated wastewater, energy efficiency becomes less relevant, because the osmotic pressure of such feedwaters, and thus the intrinsic energy for separation, are typically quite small. Consequently, other technical and practical aspects, such as selectivity, capital cost, reliability, and compatibility with intermittent operation, may deserve more considerations in future research. Notably, electrochemical desalination may have unique advantages and strong potential for selective removal of contaminants.[49−53]

In the opposite end of the salinity spectrum, the desalination of hypersaline brine, as in zero liquid discharge or treating oil and gas produced water, emerges to become a major challenge in the field. In this regime, energy efficiency becomes far more important. The current practice is mostly based on MVC, which is still energy-intensive due to the presence of phase change.[4] Other nondistillation-based approaches are being actively explored to reduce energy consumption. Notable examples include osmotically mediated RO,[54,55] multipass low-rejection RO,[56,57] and low-temperature solvent extraction.[58−60] Future research in this area should either further explore nondistillation-based desalination processes to reduce energy consumption or enable the use of low-grade thermal energy to reduce energy cost.

It is a misconception to think that all desalination processes are energy-intensive, as the energy consumption of desalination strongly depends on feed salinity. Desalination of seawater (35 g/L TDS) is indeed more energy-intensive than conventional freshwater treatment, but nonetheless still very small compared to energy consumption in other human activities.[6] A rough calculation suggests that supplying water using seawater RO to the three most populated coastal cities in the U.S. (New York, Los Angeles, and Houston, with a total population of ∼14.7 million) requires only ∼0.2% of the current U.S. energy consumption. Given the societal importance of freshwater, desalination is not prohibitively energy-intensive when and where we run out of more economical means of water supply. Lastly, while the scientific community tends to focus on technical metrics, we must understand that the consideration of energy in desalination is practically only relevant to the overall cost of water treatment, and that the value proposition for developing new desalination technologies should aim at achieving a lower overall treatment cost, not just a higher energy efficiency.

ASSOCIATED CONTENT

Supporting Information

The Supporting Information is available free of charge at https://pubs.acs.org/doi/10.1021/acs.est.9b04788.

Interpretation of "separation bar" (Section S1); Derivation of the product water-specific Gibbs free energy of separation (Section S2); Derivation of the ion-specific Gibbs free energy of separation (Section S3); Thermodynamic energy efficiency of a single-stage RO process with and without energy recovery device (Section S4); Thermodynamic energy efficiency of two-stage and three stage RO processes with and without energy recovery device (Section S5); Thermodynamic energy efficiency of electrodialysis (Section S6); Thermodynamic energy efficiency of thermal distillation (Section S7); Calculation of TEE from literature data for Figure 3 (Section S8) (PDF)

AUTHOR INFORMATION

Corresponding Author

*Phone: +1(615)322-7226; e-mail: shihong.lin@vanderbilt.edu.

ORCID

Shihong Lin: 0000-0001-9832-9127

Notes

The author declares no competing financial interest.

DOI: 10.1021/acs.est.9b04788
Environ. Sci. Technol. 2020, 54, 76−84

Biography

Dr. Shihong Lin is an assistant professor in the Department of Civil and Environmental Engineering and the Department of Chemical and Biomolecular Engineering at Vanderbilt University, Nashville. He obtained his Ph.D. (2012) and M.S. degrees from Duke University, and his B.Sc. (2006) from Harbin Institute of Technology, China, all in Environmental Engineering. Dr. Lin did his postdoc at Yale University in 2013−2014, before starting his position at Vanderbilt in 2015. He directs a research group with primary interest in advancing water treatment and desalination technologies via (1) enhancing fundamental understanding of these technologies from molecular to system level, and (2) developing new processes and materials that lead to higher efficiency, reliability, and versatility. Using both experimental and modeling techniques, Lin's research group has worked on multiple desalination technologies including reverse osmosis, nanofiltration, capacitive deionization, membrane distillation, electrodialysis, and forward osmosis. Notable recognitions Dr. Lin has received include the ACS-PRF Doctoral New Investigator Award (2016), the ORAU Ralph Powe Junior Faculty Enhancement Award (2016), and the National Academy of Engineering Frontier of Engineering Symposium Fellow (2016). He is currently the associate editor *of Journal of Water Process Engineering* under Elsevier.

■ ACKNOWLEDGMENTS

The author acknowledges the support from National Science Foundation (NSF) via standard research grant 1739884 and from Oak Ridge Associated Universities (ORAU) through the Ralph E. Powe Jr Faculty Enhancement Award.

■ REFERENCES

(1) Shannon, M. A.; Bohn, P. W.; Elimelech, M.; Georgiadis, J. G.; Mariñas, B. J.; Mayes, A. M. Science and Technology for Water Purification in the Coming Decades: Article: Nature. *Nature* **2008**, *452*, 301−310.
(2) Greenlee, L. F.; Lawler, D. F.; Freeman, B. D.; Marrot, B.; Moulin, P. Reverse Osmosis Desalination: Water Sources, Technology, and Today's Challenges. *Water Res.* **2009**, *43*, 2317−2348.
(3) Elimelech, M.; Phillip, W. A. The Future of Seawater Desalination: Energy, Technology, and the Environment. *Science* **2011**, *333*, 712−717.
(4) Tong, T.; Elimelech, M. The Global Rise of Zero Liquid Discharge for Wastewater Management: Drivers, Technologies, and Future Directions. *Environ. Sci. Technol.* **2016**, *50*, 6846−6855.
(5) Spiegler, K. S.; El-Sayed, Y. M. The Energetics of Desalination Processes. *Desalination* **2001**, *134*, 109−128.
(6) Semiat, R. Energy Issues in Desalination Processes. *Environ. Sci. Technol.* **2008**, *42*, 8193−8201.
(7) Reducing Energy Consumption in Seawater Desalination. *Desalination* **2004**, *165*, 299−312.
(8) McGinnis, R. L.; Elimelech, M. Energy Requirements of Ammonia−Carbon Dioxide Forward Osmosis Desalination. *Desalination* **2007**, *207*, 370−382.
(9) Zhao, R.; Biesheuvel, P. M.; Van der Wal, A. Energy Consumption and Constant Current Operation in Membrane Capacitive Deionization. *Energy Environ. Sci.* **2012**, *5*, 9520−9527.
(10) Brogioli, D.; La Mantia, F.; Yip, N. Y. Thermodynamic Analysis and Energy Efficiency of Thermal Desalination Processes. *Desalination* **2018**, *428*, 29−39.
(11) Spiegler, K. S.; Kedem, O. Thermodynamics of Hyperfiltration (Reverse Osmosis): Criteria for Efficient Membranes. *Desalination* **1966**, *1*, 311−326.
(12) Song, L.; Hu, J. Y.; Ong, S. L.; Ng, W. J.; Elimelech, M.; Wilf, M. Emergence of Thermodynamic Restriction and Its Implications for Full-Scale Reverse Osmosis Processes. *Desalination* **2003**, *155*, 213−228.
(13) Zhu, A.; Christofides, P. D.; Cohen, Y. Energy Consumption Optimization of Reverse Osmosis Membrane Water Desalination Subject to Feed Salinity Fluctuation. *Ind. Eng. Chem. Res.* **2009**, *48*, 9581−9589.
(14) Lienhard, J. H.; Mistry, K. H.; Sharqawy, M. H.; Thiel, G. P. Thermodynamics, Exergy, and Energy Efficiency in Desalination Systems. In *Desalination Sustainability: A Technical, Socioeconomic, and Environmental Approach*; Arafat, H. A., Ed.; Elsevier, 2017.
(15) Fritzmann, C.; Löwenberg, J.; Wintgens, T.; Melin, T. State-of-the-Art of Reverse Osmosis Desalination. *Desalination* **2007**, *216*, 1−76.
(16) Yang, Z.; Guo, H.; Tang, C. Y. The Upper Bound of Thin-Film Composite (TFC) Polyamide Membranes for Desalination. *J. Membr. Sci.* **2019**, *590*, 117297.
(17) Tanaka, Y. Chapter 1 Electrodialysis. In *Electrodialysis*; Elsevier, 2007; Vol. *12*, pp 321−381.
(18) Strathmann, H. Electrodialysis, a Mature Technology with a Multitude of New Applications. *Desalination* **2010**, *264*, 268−288.
(19) Biesheuvel, P. M.; van Limpt, B.; Van der Wal, A. Dynamic Adsorption/Desorption Process Model for Capacitive Deionization. *J. Phys. Chem. C* **2009**, *113*, 5636−5640.
(20) Suss, M. E.; Presser, V. Water Desalination with Energy Storage Electrode Materials. *Joule* **2018**, *2*, 10−15.
(21) Porada, S.; Zhao, R.; Van der Wal, A.; Presser, V.; Biesheuvel, P. M. Review on the Science and Technology of Water Desalination by Capacitive Deionization. *Prog. Mater. Sci.* **2013**, *58*, 1388−1442.
(22) Suss, M. E.; Porada, S.; Sun, X.; Biesheuvel, P. M.; Yoon, J.; Presser, V. Water Desalination via Capacitive Deionization: What Is It and What Can We Expect From It? *Energy Environ. Sci.* **2015**, *8*, 2296−2319.
(23) Van der Bruggen, B.; Vandecasteele, C. Distillation vs. Membrane Filtration: Overview of Process Evolutions in Seawater Desalination. *Desalination* **2002**, *143*, 207−218.
(24) Al-Shammiri, M.; Safar, M. Multi-Effect Distillation Plants: State of the Art. *Desalination* **1999**, *126*, 45−59.
(25) Shaffer, D. L.; Arias Chavez, L. H.; Ben-Sasson, M.; Romero-Vargas Castrillón, S.; Yip, N. Y.; Elimelech, M. Desalination and Reuse of High-Salinity Shale Gas Produced Water: Drivers, Technologies, and Future Directions. *Environ. Sci. Technol.* **2013**, *47*, 9569−9583.
(26) Deshmukh, A.; Boo, C.; Karanikola, V.; Lin, S. W.; Straub, A. P.; Tong, T.; Warsinger, D. M.; Elimelech, M. Membrane Distillation at the Water-Energy Nexus: Limits, Opportunities, and Challenges. *Energy Environ. Sci.* **2018**.*111177*
(27) Sandler, S. I. *Chemical and Engineering Thermodynamics*; Wiley, 1998.
(28) Mistry, K. H.; Hunter, H. A.; Lienhard, J. H. V. Effect of Composition and Nonideal Solution Behavior on Desalination Calculations for Mixed Electrolyte Solutions with Comparison to Seawater. *Desalination* **2013**, *318*, 34−47.
(29) Tanak, Y. Chapter 3 Membrane Characteristics and Transport Phenomena. In *Membrane Science and Technology*; Elsevier, 2007; Vol. *12*, pp 37−57.

DOI: 10.1021/acs.est.9b04788
Environ. Sci. Technol. 2020, 54, 76−84

(30) Wang, L.; Dykstra, J. E.; Lin, S. W. Energy Efficiency of Capacitive Deionization. *Environ. Sci. Technol.* **2019**, *53*, 3366−3378.
(31) Lee, J.; Kim, S.; Yoon, J. Rocking Chair Desalination Battery Based on Prussian Blue Electrodes. *ACS Omega* **2017**, *2*, 1653−1659.
(32) Qin, M.; Deshmukh, A.; Epsztein, R.; Patel, S. K.; Owoseni, O. M.; Walker, W. S.; Elimelech, M. Comparison of Energy Consumption in Desalination by Capacitive Deionization and Reverse Osmosis. *Desalination* **2019**, *455*, 100−114.
(33) Ramachandran, A.; Oyarzun, D. I.; Hawks, S. A.; Campbell, P. G.; Stadermann, M.; Santiago, J. G. Comments on "Comparison of Energy Consumption in Desalination by Capacitive Deionization and Reverse Osmosis. *Desalination* **2019**, *461*, 30−36.
(34) Qin, M.; Deshmukh, A.; Epsztein, R.; Patel, S. K.; Owoseni, O. M.; Walker, W. S.; Elimelech, M. Response to comments on "Comparison of Energy Consumption in Desalination by Capacitive Deionization and Reverse Osmosis. *Desalination* **2019**, *462*, 48−55.
(35) Li, M. Energy Consumption in Spiral-Wound Seawater Reverse Osmosis at the Thermodynamic Limit. *Ind. Eng. Chem. Res.* **2014**, *53*, 3293−3299.
(36) Lin, S.; Elimelech, M. Staged Reverse Osmosis Operation: Configurations, Energy Efficiency, and Application Potential. *Desalination* **2015**, *366*, 9−14.
(37) Efraty, A.; Barak, R. N.; Gal, Z. Closed Circuit Desalination — a New Low Energy High Recovery Technology Without Energy Recovery. *Desalin. Water Treat.* **2011**, *31*, 95−101.
(38) Warsinger, D. M.; Tow, E. W.; Nayar, K. G.; Maswadeh, L. A.; Lienhard, J. H. V. Energy Efficiency of Batch and Semi-Batch (CCRO) Reverse Osmosis Desalination. *Water Res.* **2016**, *106*, 272−282.
(39) Werber, J. R.; Deshmukh, A.; Elimelech, M. Can Batch or Semi-Batch Processes Save Energy in Reverse-Osmosis Desalination? *Desalination* **2017**, *402*, 109−122.
(40) Biesheuvel, P. M. Thermodynamic Cycle Analysis for Capacitive Deionization. *J. Colloid Interface Sci.* **2009**, *332*, 258−264.
(41) Wang, L.; Biesheuvel, P. M.; Lin, S. Reversible Thermodynamic Cycle Analysis for Capacitive Deionization with Modified Donnan Model. *J. Colloid Interface Sci.* **2018**, *512*, 522−528.
(42) Hemmatifar, A.; Ramachandran, A.; Liu, K.; Oyarzun, D. I.; Bazant, M. Z.; Santiago, J. G. Thermodynamics of Ion Separation by Electrosorption. *Environ. Sci. Technol.* **2018**, *52*, 10196−10204.
(43) Energy Recovery in Membrane Capacitive Deionization. *Environ. Sci. Technol.* **2013**, *47*, 4904−4910.
(44) Mistry, K. H.; Lienhard, J. H. Generalized Least Energy of Separation for Desalination and Other Chemical Separation Processes. *Entropy* **2013**, *15*, 2046−2080.
(45) Lin, S.; Elimelech, M. Kinetics and Energetics Trade-Off in Reverse Osmosis Desalination with Different Configurations. *Desalination*, **2016**, *402*, 42−52, .
(46) Wang, L.; Lin, S. Intrinsic Tradeoff Between Kinetic and Energetic Efficiencies in Membrane Capacitive Deionization. *Water Res.* **2018**, *129*, 394−401.
(47) Liu, S.; Smith, K. C. Quantifying the Trade-Offs Between Energy Consumption and Salt Removal Rate in Membrane-Free Cation Intercalation Desalination. *Electrochim. Acta* **2018**, *271*, 652−665.
(48) Hawks, S. A.; Ramachandran, A.; Porada, S.; Campbell, P. G.; Suss, M. E.; Biesheuvel, P. M.; Santiago, J. G.; Stadermann, M. Performance Metrics for the Objective Assessment of Capacitive Deionization Systems. *Water Res.* **2019**, *152*, 126−137.
(49) Kim, Y.-J.; Choi, J.-H. Selective Removal of Nitrate Ion Using a Novel Composite Carbon Electrode in Capacitive Deionization. *Water Res.* **2012**, *46*, 6033−6039.
(50) Tang, W.; Kovalsky, P.; He, D.; Waite, T. D. Fluoride and Nitrate Removal from Brackish Groundwaters by Batch-Mode Capacitive Deionization. *Water Res.* **2015**, *84*, 342−349.
(51) Kim, T.; Gorski, C. A.; Logan, B. E. Ammonium Removal from Domestic Wastewater Using Selective Battery Electrodes. *Environ. Sci. Technol. Lett.* **2018**, *5*, 578−583.
(52) Su, X.; Kushima, A.; Halliday, C.; Zhou, J.; Li, J.; Hatton, T. A. Electrochemically-Mediated Selective Capture of Heavy Metal Chromium and Arsenic Oxyanions From Water. *Nat. Commun.* **2018**, *9*, 1−9.
(53) Wang, L.; Lin, S. Mechanism of Selective Ion Removal in Membrane Capacitive Deionization for Water Softening. *Environ. Sci. Technol.* **2019**, *53*, 5797−5804.
(54) Bartholomew, T. V.; Mey, L.; Arena, J. T.; Siefert, N. S.; Mauter, M. S. Osmotically Assisted Reverse Osmosis for High Salinity Brine Treatment. *Desalination* **2017**, *421*, 3−11.
(55) Chen, X.; Yip, N. Y. Unlocking High-Salinity Desalination with Cascading Osmotically Mediated Reverse Osmosis: Energy and Operating Pressure Analysis. *Environ. Sci. Technol.* **2018**, *52*, 2242−2250.
(56) Ahunbay, M. G. Achieving High Water Recovery at Low Pressure in Reverse Osmosis Processes for Seawater Desalination. *Desalination* **2019**, *465*, 58−68.
(57) Wang, Z.; Deshmukh, A.; Du, Y.; Elimelech, M. Minimal and zero liquid discharge with reverse osmosis using low-salt-rejection membranes. *Water Res.* **2020**, *170*, 115317.
(58) Bajpayee, A.; Luo, T.; Muto, A.; Chen, G. Very Low Temperature Membrane-Free Desalination by Directional Solvent Extraction. *Energy Environ. Sci.* **2011**, *4*, 1672−1675.
(59) Rish, D.; Luo, S.; Kurtz, B.; Luo, T. Exceptional Ion Rejection Ability of Directional Solvent for Non-Membrane Desalination. *Appl. Phys. Lett.* **2014**, *104*, 024102.
(60) Boo, C.; Winton, R. K.; Conway, K. M.; Yip, N. Y. Membrane-Less and Non-Evaporative Desalination of Hypersaline Brines by Temperature Swing Solvent Extraction. *Environ. Sci. Technol. Lett.* **2019**, *6*, 359−364.

DOI: 10.1021/acs.est.9b04788
Environ. Sci. Technol. 2020, 54, 76−84